FERROELECTRICS
2017, VOL. 510, 16–26
https://doi.org/10.1080/00150193.2017.1326286

Polaritons in magnetoelectric multiferroics films: Switching magnon polaritons using an electric field

Vincensius Gunawan and Hendri Widiyandari

Physics Department, Diponegoro University, Tembalang, Semarang, Indonesia

ABSTRACT
We present a theoretical study of polarions on the magnetoelectric multiferroics with finite thickness (film) geometry. The multiferroics are ferroelectric-antiferromagnet with canted spin structure. Dispersion relation for surface and bulk polaritons are calculated for the case of transverse electric (TE) polarization. Example results are presented using parameters appropriate for $BaMnF_4$. It is found that bulk polaritons posses discreet character due to the film geometry. We also found that there are two branches of surface polaritons which are reciprocal. Example results for attenuated total reflection (ATR) are also presented. Analyzing the ATR reflection, we found that the branches of surface polaritons are able to be switched by applying an electric field opposite to the polarization.

ARTICLE HISTORY
Received 20 October 2016
Accepted 27 February 2017

KEYWORDS
Magnetoelectric multiferroic; switching; polaritons

1. Introduction

Electromagnetic waves which propagate in material with properties modified by elementary excitation of those material are defined as polaritons [1, 2]. Recently, there are studies of polaritons generated in magnetoelectric multiferroics [3-9]. Since fundamental excitations of this type of material consist of spin waves and lattice vibrations, one may generate magnon polaritons and phonon polaritons simultaneously [7]. The polaritons may be localized to travel at the surface of materials which are defined as surface polaritons [2].

The polaritons may show non-reciprocity where the frequency propagation is not similar under the opposite direction, $\omega(\vec{k}) \neq \omega(-\vec{k})$ [10]. The non-reciprocity of the surface polaritons had reported for ferromagnet [11], antiferromagnet [12] and also multiferroics [13]. In magnetic system, the non-reciprocity of the surface modes may be controlled using an external magnetic field. In magnetoelectric multiferroics, the non-reciprocity of the magnetic surface modes can be controlled using an external electric field which is able to flip the electric polarization [7]. In these studies, the geometry of the sample is considered as semi-infinite geometry with an infinite thickness. Since there is only one surface to be considered, the surface modes are characterized by solutions which decay exponentially within the material.

CONTACT Vincensius Gunawan goenangie@fisika.undip.ac.id

In this paper, we discuss in detail how the thickness of material affects polaritons in canted spin multiferroics with linear magnetoelectric coupling. In order to make connection to the previous study [3, 7–9, 13], we provide numerical calculation using $BaMnF_4$ as a material sample. Here, an appropriate coupling is PML type, where the electric polarization of the ferroelectric $\vec{P}$ drives the sub-lattices magnetization of the antiferromagnetic to be canted resulting in weak ferromagnetism $\vec{M}$. The dependence of the dispersion relation curves to the thickness of the material is presented. We also show that the application of an external electric field may switch the localization of the surface polaritons in finite thickness geometry.

This paper is organized as follows. The geometry and the susceptibility of the magnetoelectric multiferroics are briefly described in section 2. In section 3, The derivation of dispersion relations for both surface and bulk modes is presented and solutions are provided in section 4. Here, the possibility to control the localization of the surface modes is also discussed. Conclusions are given in section 5.

2. Geometry and susceptibility

The geometry of this study is illustrated in Figure 1. The material sample has a thickness L with the top surface is located at $z = 0$ and the bottom is set at $z = L$. The multiferroic is ferroelectric-antiferromagnetic with magnetoelectric coupling assumed to be Dzyaloshinkii-Moriya (DM) type. In this type of coupling, the spontaneous polarization induce the sub-lattices magnetization to be canted resulting in weak ferromagnetism $\vec{M}$ perpendicular to the electric polarization $\vec{P}$. Both the electric polarization and weak magnetism are confined in x-y plane.

We assume that the energy density of this material system is contributed by the ferroelectric, magnetic system and magnetoelectric coupling as [7]

$$F = F_E + F_M + F_{ME} \tag{1}$$

where the energy density of the ferroelectric F_E with spontaneous polarisation parallel to the $\widehat{y}$ is represented by a fourth order Ginzburg-Landau energy density as [7]

$$F_E = \frac{1}{2}\xi_1 P_y^2 + \frac{1}{4}\xi_2 P_y^4 + \frac{1}{2}\Delta_1\left(P_x^2 + P_z^2\right) + \frac{1}{4}\Delta_2\left(P_x^4 + P_z^2\right) - E_y P_y \tag{2}$$

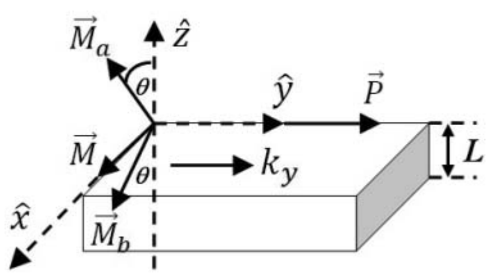

Figure 1. An illustration of the geometry. The thickness of the multiferroics is L. The polarization P causes the sub-lattices of the antiferromagnetic to be canted resulting weak ferromagnetism M. The surface polaritons propagate with wave vector k_y parallel to the electric polarization along the y axis.

Here, the electric energy density contribution of P_y component is represented by the first and second term with ξ_1 and ξ_2 are dielectric stiffness. The third and the fourth terms correspond to the energy density in x and z components with Δ_1 and Δ_2 represent stiffness constant in the related directions. The external electric $\vec{E}$ is applied parallel to the spontaneous polarization.

The magnetic energy density comprised of the exchange interaction, anisotropy interaction and Zeeman effect is represented as [7]

$$F_M = -\lambda \vec{M}a \cdot \vec{M}_b - \frac{K}{2}\left[\left(\vec{M}_a \cdot \hat{z}\right)^2 + \left(\vec{M}_b \cdot \hat{z}\right)^2\right] - \left(\vec{M}_a + \vec{M}_b\right) \cdot \vec{H}_0 \tag{3}$$

where $\vec{M}_a$ and $\vec{M}_b$ are sub-lattices magnetization. The exchange constants are represented by λ with $\boldsymbol{\lambda} > 0$. The second term corresponds to the anisotropy energy density with the anisotropy constant K. The last term is Zeeman energy density with external magnetic field H_0.

The energy density from magnetoelectric interaction with induced DM polarization is of the form [7]

$$F_{ME} = -\alpha P_y M_x L_z = -2\alpha P_y M_x^2 \sin 2\theta \tag{4}$$

where α is magnetoelectric coupling and M_x represents magnitude of the sub-lattice magnetization. Here, weak ferromagnetism M_x and antiferromagnetic vector L_z are defined as

$$M_x = \left(\vec{M}_a + \vec{M}_b\right)_x = 2M_s \sin 2\theta \tag{5}$$

and

$$L_z = \left(\vec{M}_a - \vec{M}_b\right)_x = 2M_s \cos 2\theta. \tag{6}$$

In order to obtain dispersion relation for both bulk and surface polaritons, we need to determine the magnetic and dielectric linear responses. The magnetic and electric susceptibilities are calculated from the magnetic torque equation and the Landau-Khalatnikov equation of motion. The detail of the calculations is given in Ref. [7,8], here we directly present the results which are needed for the next calculations. Since we are focusing the study on TE modes which are involving the electric field component E_x and the magnetic field components H_y and H_z, the required electric susceptibility components are

$$\chi_{xx}^e = \varepsilon_{xx}^{\infty} \frac{\omega_{L,x}^2 - \omega^2}{\omega_{T,x}^2 - \omega^2} - 1 \tag{7}$$

where $\omega_{L,x}$ and $\omega_{T,x}$ represent the longitudinal and transverse phonon resonance frequency in x direction. The magnetic susceptibility components for this modes are defined as [7]

$$\chi_{yy}^m = \frac{2\omega_s(\omega_a \cos 2\theta + 2\omega_{me} \sin 2\theta + \omega_0 \sin\theta)}{(\omega_M^2 - \omega^2)}, . \tag{8}$$

$$\chi_{zz}^m = \frac{2\omega_s(\omega_{me} \sin 2\theta + \omega_0 \sin\theta)}{(\omega_M^2 - \omega^2)}. \tag{9}$$

and

$$\chi_{yz}^m = \frac{i2\omega_s\omega \sin\theta}{(\omega_M^2 - \omega^2)}. \tag{10}$$

where magnetic resonance frequency in TE modes is defined as

$$\omega_M = \left(\omega_{afm}^2 \cos^2\theta + \Omega_{me}^2 + \Omega_0^2\right)^{1/2} \tag{11}$$

with the magnetoelectric frequency Ω_{me} and external magnetic Ω_0 are defined as

$$\Omega_{me} = [\omega_{me}(4\omega_{me} \cos\theta + \omega_a \sin 2\theta + 2\omega_{ex} \sin 2\theta)]^{1/2} \tag{12}$$

and

$$\Omega_0 = [\omega_0(\omega_0 - \omega_a \sin 2\theta + 2\omega_{me} \cos\theta)]^{1/2}. \tag{13}$$

The frequencies are described as $\omega_{ex} = \gamma\lambda M_s$ which is the frequency from exchange interaction, $\omega_a = \gamma K M_s$ which is contributed by anisotropy energy, $\omega_s = \gamma M_s$ which is contributed by sub-lattice magnetization, $\omega_{afm} = [\omega_a(\omega_a + 2\omega_{ex})]^{1/2}$ which is antiferromagnet frequency, $\omega_{me} = \gamma\alpha P_y M_s$ which is from magnetoelectric interaction and $\omega_0 = \gamma H_0$ which is Zeeman effect. The magnetic permittivity and electric permeability are related to the susceptibilities by $\mu = I + 4\pi\chi^m$ and $\varepsilon = I + 4\pi\chi^e$, where I is identity matrix.

3. Theory for bulk and surface polaritons

In finite thickness geometry (film), there are two surfaces (top and bottom) that should be considered. It means that the solution with exponentially decreasing and increasing is allowed. The formulation of the surface waves should be composed of an addition of exponentially decreasing and increasing function within the materials. Outside materials, the surface waves are only exponentially decreasing with distance. Based on the configuration in Fig. (1) where the surface modes propagate parallel along y axis, the dispersion relation for TE surface polaritons is derived by assuming solution as

$$\vec{E} = \begin{cases} \hat{x}E_0 e^{-\beta_0 z} \exp[i(k_y y - \omega t)] & z > 0 \\ \hat{x}\left(E_m e^{-\beta z} + \widetilde{E}_m e^{\beta z}\right) \exp[i(k_y y - \omega t)] & -L < z < 0 \\ \hat{x}\tilde{E}_0 e^{-\beta_0 (z - |L|)} \exp[i(k_y y - \omega t)] & z < -L \end{cases}. \tag{14}$$

Here, E_0 and $\widetilde{E}_0$ represent amplitudes of the waves outside the materials while parameters E_m and $\widetilde{E}_m$ are the amplitudes of the waves in the multiferroics. The constants β and β_0 represent the attenuation constant of the sample and vacuum which can be easily derived using

Maxwell equations resulting in an implicit equations as [7]

$$\mu_{zz}\beta^2 = \mu_{yy}k_y^2 - \varepsilon_{xx}\left(\mu_{yy}\mu_{zz} - \mu_{yz}^2\right)\frac{\omega^2}{c^2}. \tag{15}$$

and

$$\beta_0^2 = k_y^2 - \frac{\omega^2}{c^2}. \tag{16}$$

The values of the attenuation constant β determine the the type of the polaritons. They are surface polaritons if β is real, and bulk polaritons if β is imaginary. Then, considering continuity of the fields (continuity of normal induced magnetic field $\vec{B}$ and tangential magnetic field $\vec{H}$ at the top and bottom of the material), we obtain four equations with four unknown amplitudes. Solving these four equations simultaneously, we obtain implicit dispersion relation for surface polaritons as

$$\left[\left(\beta^2\mu_{zz}^2 - k_y^2\mu_{yz}^2\right) + \beta_0^2\mu_v^2\right]\tanh(\beta L) + 2\beta_0\beta\mu_{zz}\mu_v = 0. \tag{17}$$

where $\mu_v = (\mu_{yy}\mu_{zz} - \mu_{yz}^2)^{\frac{1}{2}}$. The dispersion stated by Eq. (17) expresses the reciprocal surface polaritons since the formulation is symmetry with respect to the wave vector k_y. Hence, the direction of the propagation does not matter. In film with finite thickness configuration, it is the localization of the surface polaritons which is interesting to study, as we will discuss later by analyzing the calculated attenuated total reflection.

The dispersion relation for the bulk modes could be easily obtained by changing attenuation constant $\alpha \rightarrow i\alpha$ resulting in the form

$$\left[\beta_0^2\mu_v^2 - \left(\beta^2\mu_{zz}^2 - k_y^2\mu_{yz}^2\right)\right]\tan(\beta L) + 2\beta_0\beta\mu_{zz}\mu_v = 0. \tag{18}$$

Unlike the relation dispersion for semi-infinite geometry, the formulation of the bulk modes for film contains the harmonic function which is expressed as tangential form. Hence, the bulk bands in semi-infinite geometry [7] breaking up into discrete bulk dispersion relation as it had discussed in the previous studies of ferromagnet and antiferromagnet [10]. Since there is restriction at the top and bottom, the bulk modes have approximately standing wave properties.

4. Application to multiferroic $BaMNF_4$

In this section, we are applying the above theory for multiferroic $BaMnF_4$. We calculate the dispersion relation for the case of transverse electric (TE) using parameters appropriate for $BaMnF_4$ determined as follows. We use the frequencies for magnetic system as [8,9]: magnetization frequency $\omega_s = 0.2853$$ cm^{-1}, exchange frequency $\omega_{ex} = 46.66$$ cm^{-1}, anisotropy frequency $\omega_a = 0.0961$$ cm^{-1} and magnetoelectric frequency $\omega_{me} = 0.14$$ cm^{-1}. Here, we also use the dielectric constant for x direction [3], $\varepsilon_{xx} = 8.3$.

The results of numerical calculation using above parameters for finite thickness geometry with various thicknesses: 2 mm, 5 mm, 8 mm and 10 mm are illustrated in Fig. (2). Unlike the result for semi-infinite geometry [7] where the bulk modes is continue and the surface modes are non-reciprocal, here as predicted, we obtain the results with different character. The relation dispersions of the bulk polaritons are discrete as previously discussed. Near the resonance frequency ω_m the bulk modes look continue since the most effective generation of polaritons is

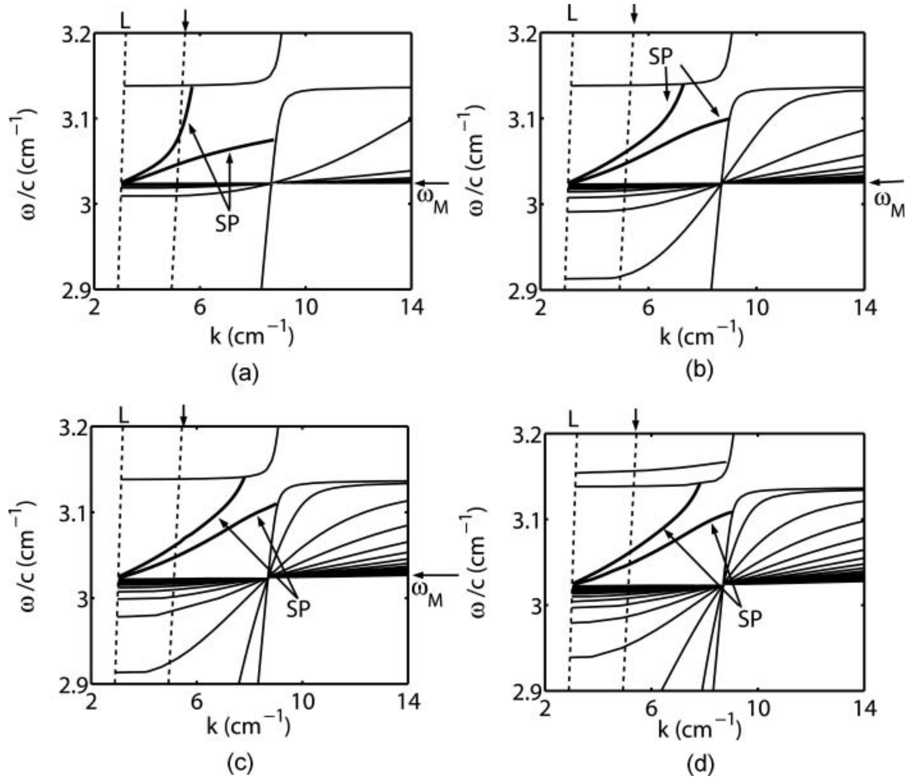

Figure 2. The dispersion relation of polaritons in magnetoelectric multiferroics films with various thicknesses. The thicknesses are: (a) 0.2 cm, (b) 0.5 cm, (c) 0.8 cm and (d) 1 cm. The thick lines denoted by 'SP' represent surface modes. A dashed line denoted by down arrow represents ATR lines with incident angle 30°.

around the resonance frequency; then the curve density of the bulk modes is high near that frequency as illustrated in Fig. (2). It can also be seen from Fig. (2a) to (2d) the curve density in bulk modes raise when the film thickness is increased. Since the bulk modes in finite thickness geometry have standing wave character with the wavevector obeys $k_y = n\pi/L$, then the number of modes increase when the thickness of multiferroics becomes thicker.

The relation dispersion for surface modes is also different from the surface polaritons in semi-infinite geometry from the previous report [7]. Unlike the surface modes in semi-infinite geometry which only have a branch of surface modes for each direction of propagation ($+k_y$ or -k_y), there are two branches of surface modes. However the upper branch of surface modes have a similar trend to the surface mode in semi-infinite geometry which propagates in positive wavevector. Also, the lower branch of surface mode is showing the similar tendency to the surface polariton in semi-infinite geometry which propagate in negative wavevector. Compared to the semi-infinite geometry, the finite thickness (film) configuration has higher order of symmetry resulting in reciprocal surface polaritons in the dispersion relation.

It is also shown in Fig. (2c) that 30° ATR line denoted by down arrow intersect with upper branch at frequency around 3.06 cm^{-1} and lower branch at frequency around 3.04 cm^{-1}. ATR is a good method to identify surface polaritons. It is used successfully to detect surface polaritons in antiferromagnet [14,15]. In ATR method, a high index prism is placed above the material sample to couple the surface excitation of the material with electromagnetic waves. By analyzing the reflectance at involved surfaces, the ATR reflectivity is derived as

$$R = \left| \frac{k_z\left(1 + r_t e^{-2\beta_0 d}\right) - i\beta_0\left(1 - r_t e^{-2\beta_0 d}\right)}{k_z\left(1 + r_t e^{-2\beta_0 d}\right) + i\beta_0\left(1 - r_t e^{-2\beta_0 d}\right)} \right| \tag{19}$$

where d represents a gap between prism and material sample while $k_z = \sqrt{\varepsilon_p}\frac{\omega}{c}\cos\theta$ is propagation normal to the surface with ε_p represents dielectric constant of the high index prism. Here, r_t is defined as reflectivity at the top surface of materials sample which is formulated as

$$r_t = \frac{\beta_0(1 + r_b) - \kappa}{\beta_0(1 + r_b) + \kappa} \tag{20}$$

where κ is defined as

$$\kappa = \left[\left(\mu_{zz}\beta - \mu_{yz}k_y\right) - \left(\mu_{zz}\beta + \mu_{yz}k_y\right)r_b\right]/\mu_v \tag{21}$$

and r_b is reflectivity at the bottom of the material sample (film) in the form

$$r_b = \frac{[(\mu_{zz}\beta - \mu_{yz}k_y) - \beta_0]}{[(\mu_{zz}\beta + \mu_{yz}k_y) + \beta_0]} e^{-2\beta L}. \tag{22}$$

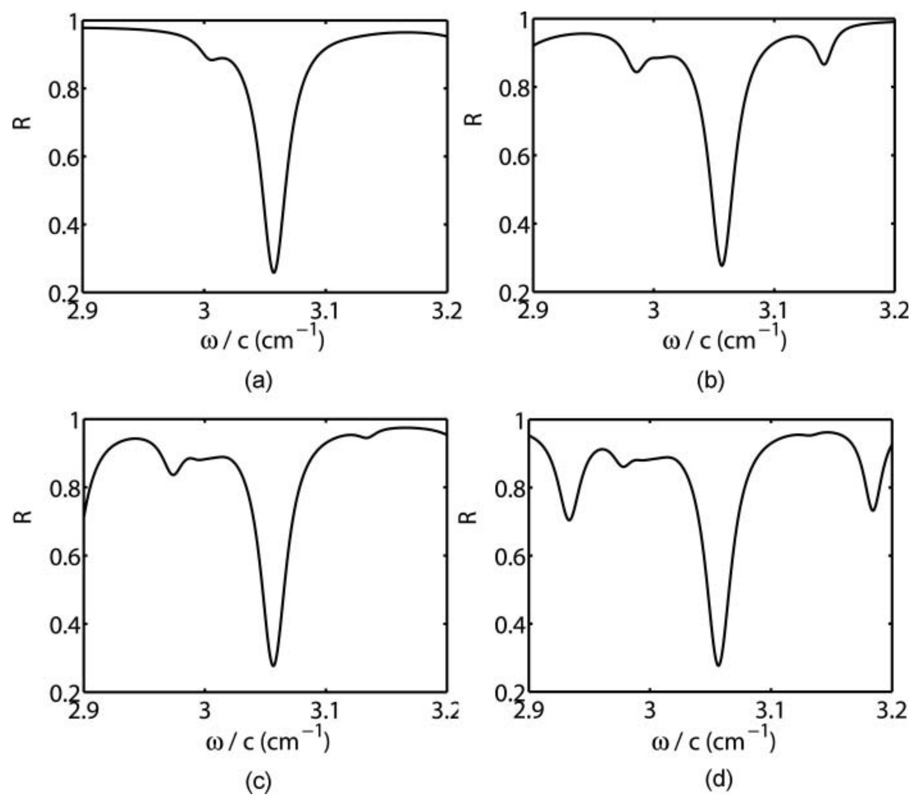

Figure 3. The calculated ATR reflection with various thicknesses. The thicknesses are: (a) 0.2 cm, (b) 0.5 cm, (c) 0.8 cm and (d) 1 cm. The sharp dips around frequency 3.06 cm^{-1} correspond to the upper branch of the surface modes.

Here, β and β_0 represent the attenuation constant of the multiferroicd and vacuum as determined in Eq. (15) and Eq. (16). Propagation parallel to the surface is represented by $k_y = \sqrt{\varepsilon_p}\frac{\omega}{c}\sin\theta$.

Calculated ATR reflectivity results for $BaMnF_4$ films are presented in Figures (3a) to (3d) for the incident angle 30° which correspond to the propagation in positive y direction. Instead of two sharp dips, the ATR spectrum only illustrate a single sharp dip. The frequencies of the sharp dips in Fig. (3a) to Fig. (3d) indicate the intersection points between ATR lines and the upper branches of the surface polaritons. Hence, it can be concluded that the upper branch surface polaritons dominate the lower branch surface polaritons in positive propagation. Considering and comparing to the previous studies [7, 10], these upper branch surface polaritons are localized and propagate at the top surface of the magnetoelectric multiferroics film.

The existence of the discrete bulk modes is indicated by the shallow dips in Fig. (3). Since the interaction between weak ferromagnetism and electromagnetic waves is delicate, the discreet character is not clearly visible in reflectivity. If the thickness of the film is increased

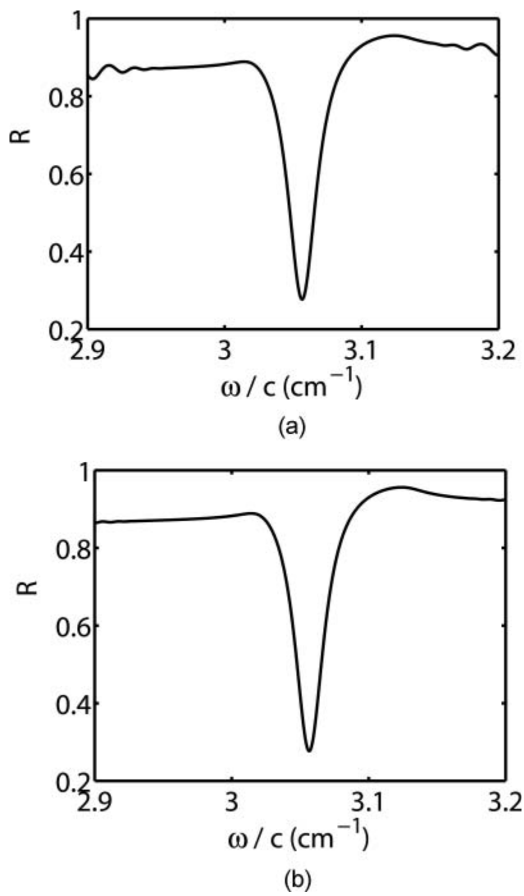

Figure 4. The calculated ATR reflection with thick films. The thicknesses are: (a) 5 cm (b) 10 cm. In the thickness 100 mm, it is found that the bulk region become smooth indicating that the bulk mode is having continue character.

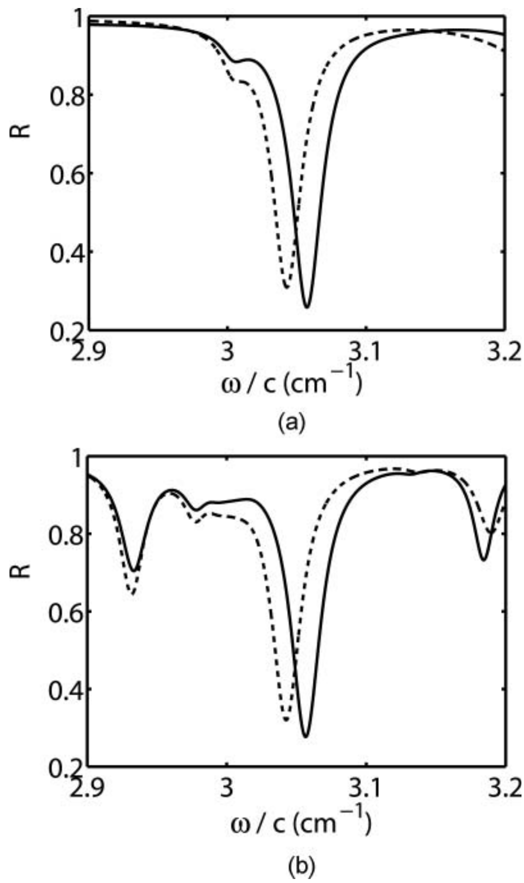

Figure 5. The ATR reflectivity for positive and negative k_y propagation of the surface modes. In (a) the thickness of the multiferroics is 0.2cm, while (b) the thickness is 1 cm. The solid lines represent surface modes with $+ k_y$ propagation, while the dashed lines are surface polaritons with - k_y propagation.

into 100 mm (see Fig. (4b), the ATR reflectivity shows that the bulk region is smooth as in previous research\cite [7] for semi-infinite configuration.

It is interesting to analyze calculated ATR with the opposite direction. Calculated ATR results for surface propagation which propagate in the y direction with incident angle -30° are presented in Figure (5) as dashed lines. There is also only one sharp dip which represents the existence of surface polaritons. Now, the frequency of the sharp dips correspond to the intersection point between lower branch surface polaritons and the ATR lines. In this direction of propagation, the lower branch surface modes are dominant. According to the Ref. [7], it can be concluded that the lower branch of the surface polaritons are localized at the bottom of the film.

Since the multiferroics materials have magnetoelectric coupling, then in principle, the TE modes polaritons which have magnetic character can be modified using an external electric fields. Since the TE modes do not have magnetoelectric susceptibility, application of the electric fields has insignificant effect. However, the interesting result is obtained when the external electric fields are applied in the opposite direction to the electric polarization and high enough (for example, -5×10^9 V/m) to flip the electric polarization. Note that we assume the materials structure does not breakdown. As a consequence, canting angle and the

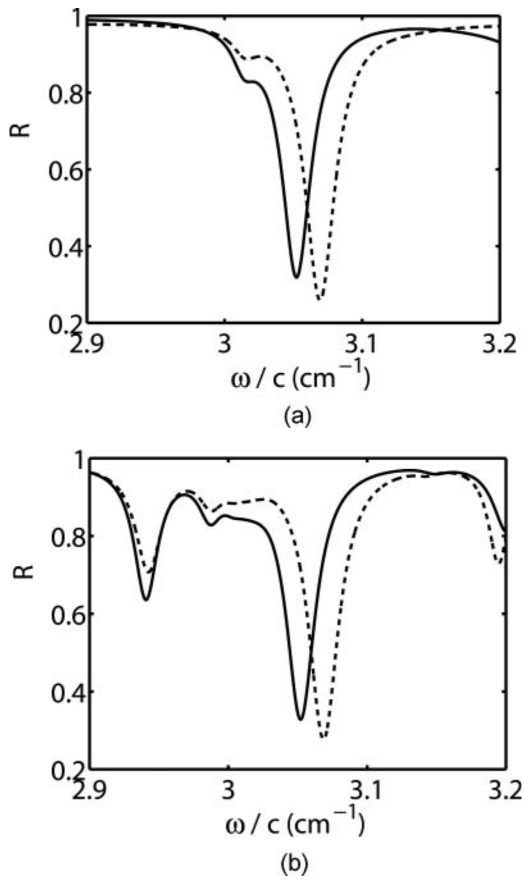

Figure 6. The ATR reflectivity of a multiferroic film with the electric polarization is flipped by an applied electric field. In (a) the thickness is 0.2 cm, while the thickness in (b) is 1 cm. The dashed lines represent the surface modes which propagate in positive k_y direction, while the solid lines are surface polaritons which propagate in negative k_y direction.

direction of the weak ferromagnetism are also flipped which in turn switch the localization of the surface modes, as illustrated in Fig. (6). Now, the surface polaritons propagate at the top surface correspond to the lower branch of the surface modes at the dispersion relation Fig. (2) At the bottom, the localized surface polaritons match up with the upper branch of surface modes in dispersion relation.

5. Conclusion

We have shown the influence of the finite thickness geometry to the properties of both bulk and surface TE polaritons. We find that restriction of the top and bottom surfaces break down the bulk modes into discreet character. This discreet property is influenced by the thickness of the film. The density of the discreet bulk modes increases when the thickness is expanded.

The dispersion relation of the surface modes is reciprocal. However, the localization of surface modes is not symmetry with respect to the direction of the propagation. The localization is affected by external electric fields through changes in the direction of weak ferromagnetism.

Funding

We wish to acknowledge the support of Kementrian Riset, Teknologi dan Pendidikan Tinggi for the funding of this research.through the scheme of Riset Fundamental.

References

1. D. L. Mills and E. Burstein, *Rep. Prog. Phys.* **37**, 817, (1974).
2. R. E. Camley and D. L. Mills, *Phys. Rev. B.* **26**, 1280, (1982).
3. J. Barnas, *J. Phys. C: Solid State Phys.* **19**, 419, (1986).
4. V. D. Buchel'nikov and V. G. Shavrov, *JETP*, **82**, 380, (1996).
5. A. S. Savchenko, S. V. Tarasenko, T. N. Tarasenko and K. N. Primak, *Low Temp. Phys*, **32**, 61, (2006).
6. A. S. Savchenko and S. V. Tarasenko, *Low Temp. Phys*, **33**, 412, (2007).
7. V. Gunawan and R. L. Stamps, *J. Phys.: Condens Matter* **23**, 105901, (2011).
8. V. Gunawan and R. L. Stamps, *J. Phys.: Condens Matter* **24**, 406003, (2012).
9. V. Gunawan and H. Widiyandari, *J. Phys.:Conf. Series*, **710**, 012037, (2016).
10. R. E. Camley, *Surf. Sci. Rep.* **7**, 103, (1987).
11. R. W. Damon and J. R. Esbach, *J. Phys. Chem. Solids*, **19**, 308, (1961).
12. L. Remer, B. Luthi, H. Sauer, R. Geick and R. E. Camley, *Phys. Rev. Lett.* **56**, 2752, (1986).
13. J. Barnas, *Phys. Stat.Sol. B*, **137**, K 43, (1986).
14. M. R. F. Jensen, T. J. Parker, K. Abraha and D. R. Tilley, *Phys. Rev. Lett.* **75**, 3756, (1995).
15. M. R. F. Jensen, S. Feiven, T. J. Parker and R. Camley, *Phys. Rev. B.* **55**, 2745, (1997).